Human Adenovirus Proteinase: DNA Binding and Stimulation of Proteinase Activity by DNA †

ARTICLE *in* BIOCHEMISTRY · DECEMBER 2001

Impact Factor: 3.02 · DOI: 10.1021/bi0111653 · Source: PubMed

7 AUTHORS, INCLUDING:

William J McGrath
Brookhaven National Laboratory
40 PUBLICATIONS **840** CITATIONS
SEE PROFILE

Mary Lynn Baniecki
Broad Institute of MIT and Harvard
20 PUBLICATIONS **323** CITATIONS
SEE PROFILE

Human Adenovirus Proteinase: DNA Binding and Stimulation of Proteinase Activity by DNA†

William J. McGrath,‡ Mary Lynn Baniecki,§ Caroline Li,‡ Sarah M. McWhirter,‡ Mark T. Brown,§ Diana L. Toledo,‡ and Walter F. Mangel*,‡

Biology Department, Brookhaven National Laboratory, Upton, New York 11973, and Department of Pharmacological Sciences, State University of New York at Stony Brook, Stony Brook, New York 11794

Received June 6, 2001; Revised Manuscript Received July 18, 2001

ABSTRACT: The interaction of the human adenovirus proteinase (AVP) with various DNAs was characterized. AVP requires two cofactors for maximal activity, the 11-amino acid residue peptide from the C-terminus of adenovirus precursor protein pVI (pVIc) and the viral DNA. DNA binding was monitored by changes in enzyme activity or by fluorescence anisotropy. The equilibrium dissociation constants for the binding of AVP and AVP−pVIc complexes to 12-mer double-stranded (ds) DNA were 63 and 2.9 nM, respectively. DNA binding was not sequence specific; the stoichiometry of binding was proportional to the length of the DNA. Three molecules of the AVP−pVIc complex bound to 18-mer dsDNA and six molecules to 36-mer dsDNA. When AVP−pVIc complexes bound to 12-mer dsDNA, two sodium ions were displaced from the DNA. A ΔG_0^0 of −4.6 kcal for the nonelectrostatic free energy of binding indicated that a substantial component of the binding free energy results from nonspecific interactions between the AVP−pVIc complex and DNA. The cofactors altered the interaction of the enzyme with the fluorogenic substrate (Leu-Arg-Gly-Gly-NH)$_2$-rhodamine. In the absence of any cofactor, the K_m was 94.8 μM and the k_{cat} was 0.002 s^{-1}. In the presence of adenovirus DNA, the K_m decreased 10-fold and the k_{cat} increased 11-fold. In the presence of pVIc, the K_m decreased 10-fold and the k_{cat} increased 118-fold. With both cofactors present, the k_{cat}/K_m ratio increased 34000-fold, compared to that with AVP alone. Binding to DNA was coincident with stimulation of proteinase activity by DNA. Although other proteinases have been shown to bind to DNA, stimulation of proteinase activity by DNA is unprecedented. A model is presented suggesting that AVP moves along the viral DNA looking for precursor protein cleavage sites much like RNA polymerase moves along DNA looking for a promoter.

Human adenovirus serotype 2 (Ad2)[1] encodes a proteinase whose activity is essential for the synthesis of infectious virus (*1*). Properties of a temperature-sensitive mutant (ts-1) indicate that one of the functions of the proteinase, after virion assembly, is to cleave six major virion precursor proteins to the mature counterparts found in wild-type virus (*2*, *3*). There are ∼70 molecules of the adenovirus proteinase per virion (*4*), and they must cleave at 3200 sites to render a virus particle infectious. The ts-1 mutation mapped to the L3 23K gene (*1*, *5*). This gene has been cloned and expressed in *Escherichia coli* (*6*−*8*) or baculovirus-infected insect cells (*9*), and the resultant 204-amino acid protein has been purified.

Recombinant human adenovirus proteinase (AVP) had little activity, and that prompted a search for cofactors. One cofactor was pVIc, the 11-amino acid residue peptide from the C-terminus of adenovirus precursor protein pVI (*6*, *9*). Its sequence is GVQSLKRRRCF. The four amino acid residues preceding pVIc in pVI constitute part of an AVP consensus cleavage sequence, implying that AVP can cleave out its own cofactor. A second cofactor was the viral DNA (*6*). A crystal structure of an AVP−pVIc complex has been determined to 2.6 Å resolution (*10*). The crystal structure revealed AVP to be the first member of a new family of cysteine proteinases. In the crystal structure, the penultimate amino acid residue in pVIc formed a disulfide bond with Cys104 of AVP.

The interaction of AVP with Ad2 DNA as a cofactor is not dependent upon a specific nucleic acid sequence. Various polymers were substituted for Ad2 DNA and assayed for cofactor activity (*6*). Not only did T7 DNA substitute for Ad2 DNA, but single-stranded DNAs, circular single- and double-stranded DNAs, transfer RNAs, and even polyglutamic acid also stimulated enzyme activity. The data are

† Research supported by the Office of Biological and Environmental Research of the U.S. Department of Energy under Prime Contract DE-AC0298CH10886 with Brookhaven National Laboratory, and by National Institutes of Health Grant AI41599. C.L. and S.M.M. were supported by the Department of Energy's Office of Science Education and Technical Information, as Science and Engineering Research Semester Program participants.

* To whom correspondence should be addressed: Biology Department, Brookhaven National Laboratory, 50 Bell Ave., P.O. Box 5000, Upton, NY 11973. Telephone: (631) 344-3373. Fax: (631) 344-3407. E-mail: Mangel@bnl.gov.

‡ Brookhaven National Laboratory.

§ State University of New York at Stony Brook.

[1] Abbreviations: Ad2, human adenovirus serotype 2; AVP, recombinant adenovirus proteinase; AVP−pVIc, 1:1 reversible complex of AVP with pVIc; dsDNA, double-stranded DNA; pVI, precursor to virion protein VI; pVIc, 11-amino acid residue peptide (GVQSLKRRRCF) from the C-terminus of pVI; ssDNA, single-stranded DNA; ts-1, human adenovirus temperature-sensitive mutant 1.

10.1021/bi0111653 CCC: $20.00
Published on Web 10/12/2001

consistent with the conclusion that this cofactor requirement is for a polymer with high negative charge density. Monomeric units of polymers with high negative charge density, e.g., the four deoxyribonucleoside monophosphates or glutamic acid, did not substitute for Ad2 DNA. The major polyanion with a high negative charge density in the virus particle is, of course, the viral DNA.

Here the interactions of AVP, pVIc, and AVP−pVIc complexes with different DNAs were quantitatively characterized. Binding interactions were monitored by two different techniques. The amount of ligand bound to DNA was measured by fluorescence anisotropy in which binding to DNA labeled with fluorescein was signified by a change in anisotropy. Alternatively, the binding of AVP and of AVP−pVIc complexes to DNA was monitored by the increase in proteinase activity. The AVP−pVIc complex was shown to bind to DNA, and binding of the AVP−pVIc complex to DNA was shown to be coincident with stimulation of enzyme activity by DNA.

MATERIALS AND METHODS

Materials. pVIc (GVQSLKRRRCF) was purchased from Research Genetics (Huntsville, AL). The single-stranded (ss) 12-mer DNA, the 5′-fluorescein-labeled 12-mer ssDNA (GACGACTAGGAT), the 18-mer ssDNA (GAGGACTAGGATCGTAAG), the 36-mer ssDNA (GATTGCATGATTAGAGTGTGCTGGATGTGATAGTGA), and the strands complementary to these DNAs were purchased from Life Technologies (Rockville, MD). Ellman's reagent, 5,5′-dithiobis(2-nitrobenzoate) or DTNB, and Ad2 DNA were purchased from Sigma Chemical Co. (St. Louis, MO). Octyl glucoside was purchased from Fisher Scientific (Faden, NJ). The fluorogenic substrate (Leu-Arg-Gly-Gly-NH)$_2$-rhodamine was synthesized and purified as described previously (*6*, *11*). AVP was purified as described previously (*6*, *12*).

Protein Concentrations. Protein concentrations were determined using the BCA protein assay from Pierce Chemical Co. (Rockford, IL). For the concentration of AVP, a calculated molar absorbance coefficient at 280 nm of 26 510 M^{-1} cm^{-1} was used (*13*). The concentration of pVIc was determined by titration of its cysteine residue with Ellman's reagent. A molar extinction coefficient at 412 nm of 14 150 M^{-1} cm^{-1} was used to calculate the concentration of thionitrobenzoate (*14*).

Annealing of Complementary DNAs. Double-stranded DNAs (dsDNA) were obtained by annealing complementary ssDNAs in 10 mM sodium cacodylate (pH 7.0) and 500 mM NaCl in a Perkin-Elmer Cetus DNA thermal cycler. The annealing solution was held at an initial temperature of 94 °C for 1 min and then at 72 °C for 1 min, followed by a slow cooling to 4 °C. The efficiency of annealing was determined by gel electrophoresis in a 15% polyacrylamide gel. The primary stain was ethidium bromide and the secondary stain 1% (w/v) methylene blue. Only dsDNA preparations that contained no detectable ssDNA molecules were used in these studies. The oligonucleotides were stored at −20 °C. All assays with 12-mer dsDNA were performed at 25 °C, as opposed to 37 °C, to ensure the DNA remained double-stranded. Periodically, the dsDNAs were checked by gel electrophoresis to make sure the strands remained annealed.

Formation of AVP−pVIc Complexes. Complexes of AVP with pVIc (AVP−pVIc) were formed by incubating 25 μM AVP with 65 μM dimeric pVIc in 10 mM Tris-HCl (pH 8.0) overnight at 4 °C.

Activity Assays. Assays for determining equilibrium dissociation constants, K_d, by enzyme activity contained the following in 1 mL: 10 mM Tris-HCl (pH 8.0), 2 mM octyl glucoside, the fluorogenic substrate (Leu-Arg-Gly-Gly-NH)$_2$-rhodamine, DNA, and AVP−pVIc. Assay mixtures were preincubated for 5 min at 25 °C prior to the addition of the fluorogenic substrate. The increase in fluorescence at 25 °C was monitored as a function of time in an ISS (Urbana, IL) PC-1 spectrofluorometer. The excitation wavelength was 492 nm and the emission wavelength 523 nm, both set with a band-pass of 8 nm. Assays with ssDNA contained 5 nM AVP−pVIc and 15 μM fluorogenic substrate; the DNA concentration was varied. Assays with dsDNA contained 10 nM DNA and 5 μM fluorogenic substrate; the AVP−pVIc concentration was varied.

Assays for measuring the K_m and k_{cat} in the presence of DNA were performed in 10 mM Tris-HCl (pH 8.0), 2 mM octyl glucoside, a DNA concentration 5-fold greater than the K_d, and 21 nM AVP−pVIc. Assay mixtures were preincubated for 5 min at 25 °C prior to the addition of fluorogenic substrate. The concentration of fluorogenic substrate was varied from $^1/_5$th to 5 times the K_m. Assays were also performed with our rhodamine-based substrate but using the conditions of Webster et al. (*15*): 25 mM Tris-HCl (pH 8.0), 1.0 mM EDTA, 25 nM AVP, 1.5 μM pVIc, and either 600 ng/mL Ad2 DNA or no DNA. Reactants without substrate were preincubated for 15 min at room temperature. Substrate was added, 50 μM (Leu-Arg-Gly-Gly-NH)$_2$-rhodamine, and the increase in fluorescence measured at 37 °C.

Calculating the K_d for the Binding of AVP−pVIc to 12-mer ds- and ssDNA by Enzyme Activity. The K_d for the binding of AVP−pVIc to 12-mer dsDNA was determined as follows. Increasing concentrations of AVP−pVIc, $[AVP-pVIc]_i$, were added to a constant amount of DNA, $[DNA]_o$. After 5 min at 25 °C, substrate was added and the increase in fluorescence with time, F_i, measured. A plot of F_i versus $[AVP-pVIc]_i$ yields a rectangular hyperbola. From this graph, the concentration of AVP−pVIc bound, $[AVP-pVIc]_b$, can be obtained:

$$[AVP-pVIc]_b = [DNA]_o(F_i/F_{max})$$

where F_{max} is the maximal rate of substrate hydrolysis, i.e., the rate when the DNA is saturated with AVP−pVIc. The concentration of AVP−pVIc free, $[AVP-pVIc]_f$, is

$$[AVP-pVIc]_f = [AVP-pVIc]_i - [AVP-pVIc]_b$$

From a plot of $[AVP-pVIc]_b$ versus $[AVP-pVIc]_f$, the K_d can be calculated.

The equilibrium dissociation constant, K_d, for the binding of AVP−pVIc to 12-mer ssDNA was determined as follows. Increasing concentrations of 12-mer ssDNA, $[12\text{-mer ssDNA}]_i$, were added to a constant amount of AVP−pVIc $[AVP-pVIc]_o$. After 5 min at 25 °C, substrate was added and the increase in fluorescence with time, F_i, measured. The rest of the analysis for determining K_d is the same as

that described above except that [12-mer ssDNA] is substituted for [AVP−pVIc] and $[DNA]_o$ is substituted for $[AVP-pVIc]_o$.

Fluorescence Anisotropy. Fluorescence anisotropy experiments for assessing the binding of ligand to DNA were performed at 25 °C in the thermostated sample compartment of an ISS PC-1 spectrofluorometer. An Oriel 530 nm band-pass filter was inserted before the emission photomultiplier. The excitation wavelength was 490 nm. All slit widths were set to 8 nm. The fluorescence intensity parallel and perpendicular to the incident light were measured.

Fluorescence Anisotropy Experiments for Determining K_d Values for the Binding of AVP, pVIc, and AVP−pVIc to 12-mer ss- and dsDNA. The anisotropy of 10 nM fluorescein-labeled 12-mer ssDNA in 10 mM Tris-HCl (pH 8.0) and 2 mM octyl glucoside was measured. Then, to determine the K_d, an aliquot of the ligand was added. After binding equilibrium had been reached, usually within 2 min, the change in anisotropy was measured. A second aliquot was added and the process repeated until no further change in anisotropy was observed. To determine the K_d for the binding of AVP−pVIc to 12-mer dsDNA, different concentrations of AVP−pVIc were added to solutions of 2.5 nM fluorescein-labeled 12-mer dsDNA in 10 mM Tris-HCl (pH 8.0) and 2 mM octyl glucoside. After 4 min, to allow binding equilibrium to be reached, the changes in anisotropy were measured.

Calculating K_d Values for the Binding of AVP, pVIc, or AVP−pVIc to 12-mer ds- and ssDNA by Fluorescence Anisotropy. The K_d was calculated from the fluorescence anisotropy data as follows. The anisotropy, r, is defined as

$$r = (I_{||} - GI_{\perp})(I_{||} + 2GI_{\perp})^{-1}$$

where $I_{||}$ and $I_{\perp}$ are the fluorescence emission intensities with polarizers parallel and perpendicular, respectively, to that of the exciting beam. The instrument correction factor G was determined for each experiment by measuring the $I_{\perp}/I_{||}$ ratio from horizontally polarized light. The anisotropy when the DNA is saturated with ligand, r_{max}, was determined empirically; increasing concentrations of ligand were added to a constant concentration of labeled DNA until further addition of the ligand resulted in no further change in anisotropy. The fraction of ligand bound, f_b, at any ligand concentration is

$$f_b = (r_{obs} - r_o)/(r_{max} - r_o) \text{ and } f_f = 1 - f_b$$

where r_o is the initial anisotropy of the DNA in the absence of other components and r_{obs} is the anisotropy at the specific ligand concentration. The concentrations of free ligand, L_f, and bound ligand, L_b, are

$$L_f = L_i - L_b \text{ and } L_b = f_b[DNA]$$

where [DNA] is the molar concentration of DNA molecules, and L_i is the initial concentration of ligand. From a plot of L_f versus L_b, the K_d was determined by standard methods.

Nonelectrostatic Free Energy of Binding of AVP−pVIc to 12-mer dsDNA. Fluorescence anisotropy was also used to determine the equilibrium association constants, K_A, for AVP−pVIc binding to DNA as a function of the NaCl concentration. Binding assays were carried out at 25 °C in solutions initially containing 1.8 mL of 10 mM Tris-HCl (pH 8.0), 2 mM octyl glucoside, 10 nM 5′-fluorescein-labeled 12-mer dsDNA, and either 0, 10, 20, 30, or 40 mM NaCl. The anisotropy of the solutions in the absence of ligand was determined at each NaCl concentration. Then, AVP−pVIc complexes were added, and after binding equilibrium had been reached, 2 min, the change in anisotropy was measured. This process was repeated until saturation curves were obtained. At each concentration of NaCl of <30 mM, the concentration of AVP−pVIc varied from 0.2 to 5 times the calculated K_A. At higher concentrations of NaCl, the AVP−pVIc concentration varied from 0.2 to 2 times the calculated K_A. K_A was calculated as described above for calculating the K_d, where $K_A = 1/K_d$.

Lifetimes of the Excited State. The lifetime of the excited state of the fluorescein moiety was measured in an SLM 4800 spectrofluorometer using an excitation wavelength of 490 nm and an Oriel 530 nm band-pass filter before the emission photomultiplier. The phase shift method with a frequency modulator tank filled with 19% ethanol to generate sinusoidally varying excitation light was used (*16*). All measurements were taken at a setting of 18 MHz in solutions of 25 mM Hepes (pH 8.0) containing 12.5 nM 18-mer dsDNA labeled at one of its 5′-ends with fluorescein in the absence or presence of 235 nM AVP−pVIc.

Stoichiometry of Binding of AVP−pVIc to DNA. The number of AVP−pVIc binding sites per DNA molecule was measured by activity assays under tight binding conditions, i.e., under conditions in which the concentration of DNA was 10-fold greater than the K_d. The stoichiometry of binding of AVP−pVIc to 12-mer dsDNA was also determined by fluorescence anisotropy, at a DNA concentration 20-fold greater than the K_d.

RESULTS

Stimulation of AVP−pVIc by 12-mer dsDNA. DNA is a cofactor, because it stimulates the rate of substrate hydrolysis by AVP and by AVP−pVIc. Increasing amounts of 12-mer dsDNA were added to a constant amount of AVP−pVIc, and after 5 min at 25 °C, the fluorogenic substrate (Leu-Arg-Gly-Gly-NH)$_2$-rhodamine was added. The increase in fluorescence, from the formation of the product (Leu-Arg-Gly-Gly-NH)-rhodamine, was measured as a function of time. The results are shown in Figure 1. In the absence of DNA, the rate of substrate hydrolysis was relatively low. For each concentration of DNA, the increase in fluorescence with time was linear. The rate of substrate hydrolysis increased with increasing DNA concentrations. At higher DNA concentrations, the rate of substrate hydrolysis approached a plateau, implying that the enzyme complex could be saturated with DNA.

K_d for the Binding of AVP to 12-mer ds- and ssDNA Measured by Fluorescence Anisotropy. The K_d for the binding of AVP to 12-mer dsDNA was determined by fluorescence anisotropy. Aliquots of AVP were added to a solution of 12-mer dsDNA in which one of the strands was labeled at its 5′-end with fluorescein, and the K_d was determined as described in Materials and Methods. The data are presented in Figure 2A as $[AVP]_{bound}$ versus $[AVP]_{free}$. Assuming the stoichiometry of binding of AVP to 12-mer

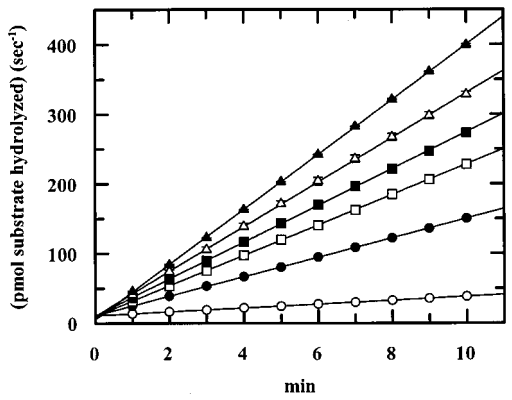

FIGURE 1: Stimulation of AVP−pVIc activity by DNA. Assays were performed with 150 nM AVP−pVIc and the indicated concentrations of 12-mer dsDNA: 0 (○), 25 (●), 50 (□), 75 (■), 100 (△), and 200 nM (▲).

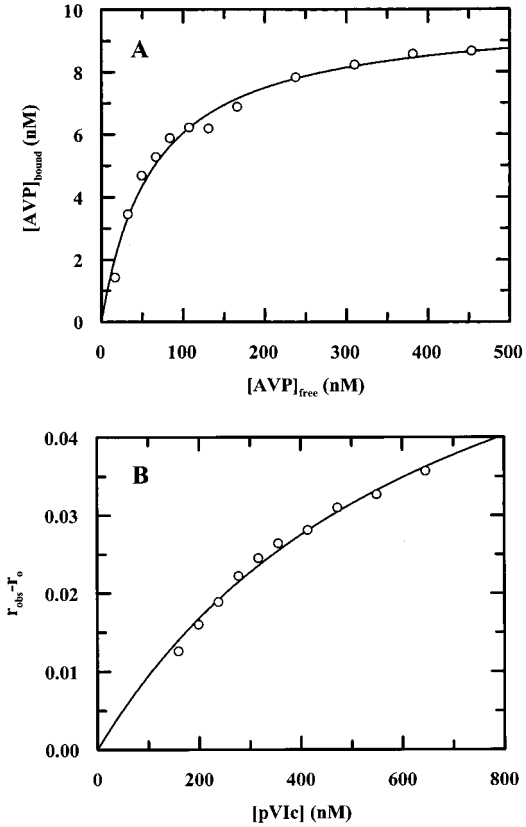

FIGURE 2: K_d for the binding of AVP to 12-mer dsDNA by fluorescence anisotropy (A) and for the binding of pVIc to 12-mer dsDNA by fluorescence anisotropy (B). (A) Increasing concentrations of AVP were added to 10 nM 5′-fluorescein-labeled 12-mer dsDNA at 25 °C. Two minutes after each addition, the change in anisotropy was measured. (B) Increasing concentrations of pVIc were added to 10 nM 5′-fluorescein-labeled 12-mer dsDNA at 25 °C. Two minutes after each addition, the change in anisotropy was measured.

dsDNA was 1:1, we found a K_d of 63 nM (Table 1). The K_d for the binding of AVP to 12-mer ssDNA was 109 nM (data not shown).

K_d for the Binding of pVIc to 12-mer ds- and ssDNA Measured by Fluorescence Anisotropy. pVIc alone, in the absence of AVP, binds to DNA. The $K_{d(apparent)}$ for the binding of pVIc to 12-mer dsDNA was determined by fluorescence anisotropy. A graph of $r_{obs} - r_o$ versus [pVIc] is shown in Figure 2B. The $K_{d(apparent)}$ was 693 nM (Table 1). The

Table 1: Equilibrium Dissociation Constants for the Binding of AVP, pVIc, and the AVP−pVIc Complex to Single- or Double-Stranded 12-mer DNA Determined by Enzyme Activity or Fluorescence Anisotropy

protein (12-mer)	K_d (nM) activity	K_d (nM) anisotropy
AVP		
(dsDNA)	−	63.08 ± 5.79
(ssDNA)		109.17 ± 15.60
pVIc		
(dsDNA)	−	693.0 ± 84.47[a]
(ssDNA)		190.4 ± 34.37[a]
AVP−pVIc		
(dsDNA)	2.92 ± 1.04	4.56 ± 2.32
(ssDNA)	18.04 ± 5.08	18.40 ± 2.80

[a] $K_{d(apparent)}$.

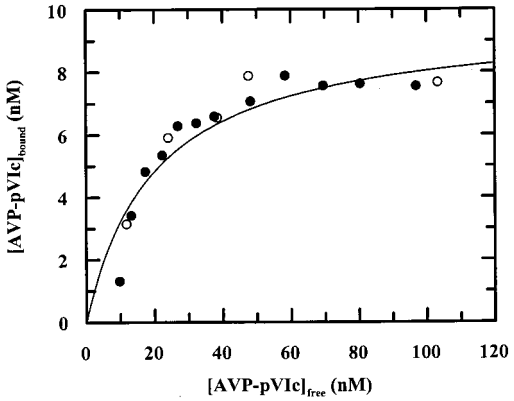

FIGURE 3: Binding to DNA by AVP−pVIc is coincident with stimulation of enzyme activity by DNA. Increasing concentrations of AVP−pVIc were added to 10 nM 5′-fluorescein-labeled 12-mer ssDNA at 25 °C. Two minutes after each addition, the change in anisotropy was measured (●). Increasing concentrations of AVP−pVIc were added to 10 nM 12-mer ssDNA. After 5 min at 25 °C, substrate was added, and the increase in fluorescence with time was measured (○). The concentrations of AVP−pVIc bound, $[AVP-pVIc]_{bound}$, and AVP−pVIc free, $[AVP-pVIc]_{free}$, were determined as described in Materials and Methods.

$K_{d(apparent)}$ for the binding of pVIc to 12-mer ssDNA was 190 nM (data not shown).

K_d for the Binding of AVP−pVIc to 12-mer ss- and dsDNA by Fluorescence Anisotropy. The K_d for the binding of AVP−pVIc to 12-mer ssDNA was obtained by fluorescence anisotropy. A graph of $[AVP-pVIc]_{bound}$ versus $[AVP-pVIc]_{free}$ is shown in Figure 3. The K_d was 18.4 nM (Table 1). The K_d for the binding of AVP−pVIc to 12-mer dsDNA was 4.6 nM (data not shown).

K_d for the Binding of AVP−pVIc to 12-mer ss- and dsDNA by Enzyme Activity. A different method was also used to obtain the K_d for the binding of AVP−pVIc to 12-mer ss- and dsDNA enzyme activity measurements. Here, increasing concentrations of AVP−pVIc were added to a constant amount of 12-mer ssDNA. After 5 min at 25 °C, substrate was added, and the increase in fluorescence with time was measured. A plot of the rate of substrate hydrolysis versus the concentration of AVP−pVIc yielded a rectangular hyperbola (data not shown). These data were subsequently converted to the concentration of AVP−pVIc bound to DNA, $[AVP-pVIc]_b$, and the free concentration of AVP−pVIc, $[AVP-pVIc]_f$. A plot of $[AVP-pVIc]_b$ versus $[AVP-pVIc]_f$ yielded a rectangular hyperbola (Figure 3). From this graph,

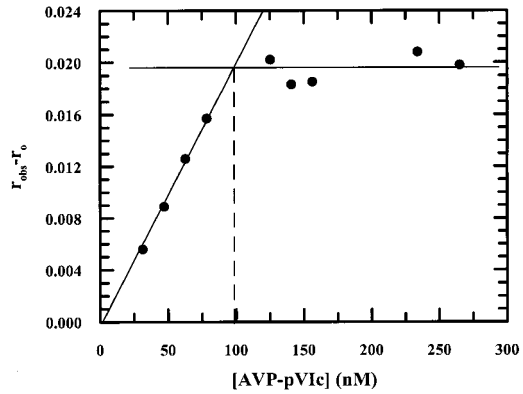

FIGURE 4: Stoichiometry of binding of AVP−pVIc to 12-mer dsDNA. Increasing concentrations of AVP−pVIc were added to 100 nM 5′-fluorescein-labeled 12-mer dsDNA at 25 °C. Two minutes after each addition, the change in anisotropy ($r_{obs} - r_o$) was measured. The two straight lines were drawn with a curve fitting routine. The dashed line is drawn from the intersection of the two straight lines to the abscissa.

Table 2: Equilibrium Dissociation Constants, K_d, and Stoichiometries of Binding of AVP−pVIc to Different DNAs Determined by Enzyme Activity

	12-mer	18-mer	36-mer	Ad2
K_d (nM)[a]				
ds	2.92 ± 1.04	5.97 ± 1.09[b]	4.65 ± 2.16[b]	−
ss	18.04 ± 5.08	8.88 ± 1.93[b]	2.13 ± 0.41[b]	
stoichiometry[c]				
ds	1:1	3:1	6:1	3027:1
ss	1:1	3:1	6:1	

[a] In units of molecules. [b] $K_{d(apparent)}$. [c] Number of AVP−pVIc molecules binding per DNA molecule.

the K_d for the binding of AVP−pVIc to 12-mer ssDNA was 18 nM (Table 1). The K_d for the binding of AVP−pVIc to 12-mer dsDNA was 2.92 nM.

Stoichiometry of Binding of AVP−pVIc to 12-mer dsDNA. Fluorescence anisotropy, under tight binding conditions, was used to ascertain the stoichiometry of binding. Increasing amounts of AVP−pVIc were added to a constant amount of 5′-fluorescein-labeled 12-mer dsDNA, and the change in anisotropy was measured. The concentration of fluorescein-labeled 12-mer dsDNA was 100 nM, 20 times the K_d determined with this technique. Under these tight binding conditions, below saturation of DNA, all AVP−pVIc present will be bound to DNA; above saturation, no added AVP−pVIc will be able to bind to DNA. The data are shown in Figure 4. As the concentration of AVP−pVIc was increased, the anisotropy increased linearly. Once saturation was reached, there was no further increase in anisotropy as additional AVP−pVIc was added. The data points could be characterized as two straight lines by a linear fitting routine. The intersection point of the two lines is the minimal concentration of AVP−pVIc required to saturate 100 nM DNA. Since that concentration of AVP−pVIc was 100 nM, the stoichiometry of binding of AVP−pVIc to 12-mer dsDNA was 1:1, one enzyme molecule per DNA molecule. An identical conclusion in a similar experiment was reached with AVP−pVIc binding to 12-mer ssDNA (Table 2).

Stoichiometry of Binding of AVP−pVIc to 18- and 36-mer dsDNA and to Ad2 DNA Determined by Enzyme Activity. The stoichiometry of binding of AVP−pVIc to 18- and 36-mer dsDNAs and to genomic Ad2 DNA was also determined under tight binding conditions, as described above with 12-mer dsDNA (Table 2). AVP−pVIc bound to 18-mer dsDNA with a 3:1 stoichiometry, to 36-mer dsDNA with a 6:1 stoichiometry, and to Ad2 DNA with a 3027:1 stoichiometry. Thus, the stoichiometry of binding was dependent upon the length of the DNA molecule. By dividing the number of base pairs per DNA molecule by the maximal number of AVP−pVIc molecules that bind to that DNA, we can calculate the number of base pairs per AVP−pVIc molecule; it is 12 with 12-mer dsDNA, 6 with 18- and 36-mer dsDNA, and 12 with Ad2 DNA.

Table 3: Effect of Cofactors on the Macroscopic Kinetic Constants for Substrate Hydrolysis[a]

	K_m (μM)	k_{cat} ($\times 10^3$ s^{-1})	k_{cat}/K_m (M^{-1} s^{-1})	relative k_{cat}/K_m
AVP	94.8 ± 7.0	2.3 ± 0.1	24.3	1
AVP−DNA	9.2 ± 1.4	24.8 ± 1.9	2700	110
AVP−pVIc	9.9 ± 1.3	271 ± 32.2	27400	1130
AVP−pVIc−DNA	3.4 ± 1.4	2780 ± 322	828000	34100

[a] Adenoviral DNA was used.

Cofactors Alter the Macroscopic Kinetic Constants for Substrate Hydrolysis. Binding of the cofactors to AVP alters the interaction of the enzyme with the fluorogenic substrate $(Leu\text{-}Arg\text{-}Gly\text{-}Gly\text{-}NH)_2$-rhodamine. In the absence of any cofactor, the K_m was 94.8 μM and the k_{cat} was 0.002 s^{-1} (Table 3). In the presence of a saturating amount of Ad2 DNA, the K_m decreased 10-fold and the k_{cat} increased 11-fold; in the presence of a saturating amount of pVIc, the K_m decreased 10-fold and the k_{cat} increased 118-fold. With both cofactors present, the k_{cat}/K_m ratio increased 34000-fold compared to that for AVP alone.

Difficulties in Observing Stimulation of AVP Activity by DNA. Webster et al. (*9*, *15*) did not see stimulation of AVP activity by DNA. Perhaps this is due to differences between their assay conditions and ours. Their substrate was the peptide MSGG↓AFSW, where cleavage occurred at the arrow; cleavage was monitored by HPLC. We repeated several of their experiments using their assay conditions but with our substrate. A rate of substrate hydrolysis of 7.2 pmol/s was observed with AVP−pVIc, and this increased 6.5-fold upon addition of 600 ng/mL Ad2 DNA (Figure 5). Under our assay conditions, after we determined the optimal concentrations of pVIc, Ad2 DNA, and substrate, a rate of substrate hydrolysis of 437 pmol/s was obtained, a rate almost 10-fold greater than that determined under their conditions in the presence of DNA.

Control Experiments for DNA Binding Measured by Anisotropy. Several control experiments were performed to ensure that in the fluorescence anisotropy experiments the binding of ligand to DNA was indeed being assessed. For the conclusions in the fluorescence anisotropy experiments to be valid, the lifetime of the excited state of the fluorophore must not change during the assay. The lifetime of the excited state of the fluorescein moiety attached to one of the 5′-ends of 18-mer dsDNA was 2.3 ± 0.4 ns, and it did not change by more than 10% when the DNA was saturated with ligand (data not shown). As a control, the lifetime of the excited state of free fluorescein was measured using as a standard reference scattering solution 0.1% (w/v) magnesium oxide. Free fluorescein consistently gave a lifetime of 3.7 ± 0.9 ns. Each lifetime measurement was the average

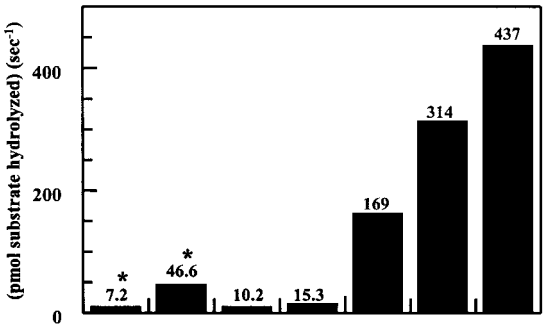

pVIc (μM)	1.5	1.5	1.5	20	1.5	1.5	1.5
Ad2 (ng/ml)	----	600	----	----	600	600	266
Substrate (μM)	50	50	50	50	50	3	3
Stimulation	1.0	6.5	1.0	1.5	16.0	20.5	43.0

* Assay conditions from Webster, et al., 1994 (15)

FIGURE 5: Effect of assay conditions on the stimulation of AVP−pVIc activity by DNA. Assays were performed with the fluorogenic substrate (Leu-Arg-Gly-Gly-NH)$_2$-rhodamine (*12*) but using the conditions defined by Webster et al. (*15*) [25 mM Tris (pH 8.0), 1.0 mM EDTA, 50 μM substrate, and 25 nM AVP]. The reactants without substrate were preincubated for 15 min at room temperature; substrate was added, and the rate of substrate hydrolysis was determined at 37 °C. Assays were also performed under the conditions described here [10 mM Tris (pH 8.0), 2 mM octyl glucoside, and 25 nM AVP]. Reactants without substrate were preincubated for 4 min at 37 °C before the addition of substrate. The bars represent the rate of substrate hydrolysis vs the assay conditions.

of 10 readings. Another indication that the ligands were binding to DNA was that changes in anisotropy were sensitive to the presence of sodium dodecyl sulfate or NaCl. If DNA saturated with ligand was incubated in either 5% sodium dodecyl sulfate or 200 mM NaCl, the anisotropy returned to its value in the absence of ligand. Last, the ligands that bound to DNA were not binding to the fluorescein moiety on DNA. When a constant amount of AVP−pVIc and fluorescein-labeled 18-mer dsDNA were incubated with increasing amounts of unlabeled 18-mer dsDNA, the change in anisotropy decreased in proportion to the amount of unlabeled 18-mer dsDNA added (data not shown). This signified competition between fluorescein-labeled 18-mer dsDNA and unlabeled 18-mer dsDNA for binding sites on AVP−pVIc and implied that AVP−pVIc was not binding to the fluorescein moiety on DNA.

Nonelectrostatic Free Energy of Binding of AVP−pVIc to dsDNA. The number of ion pairs involved in binding of AVP−pVIc to DNA was obtained by incubating 12-mer dsDNA labeled at its 5′-end with fluorescein with increasing concentrations of AVP−pVIc and determining by fluorescence anisotropy the equilibrium association constants (K_A) at different concentrations of NaCl (data not shown). The log K_A was plotted versus −log[NaCl] (Figure 6). The following equation describes the resultant straight line:

$$-\frac{\partial[\log(K_A)]}{\partial[\log(M^+)]} = m'\psi$$

where M^+ is the monovalent counterion concentration, m' is the number of ion pairs formed, and ψ is the fraction of a counterion associated, in the thermodynamic sense, with each phosphate of DNA in solution. For dsDNA, ψ is 0.88 (*17*). The number of ion pairs formed upon binding of an AVP−pVIc complex to 12-mer dsDNA was 2.18.

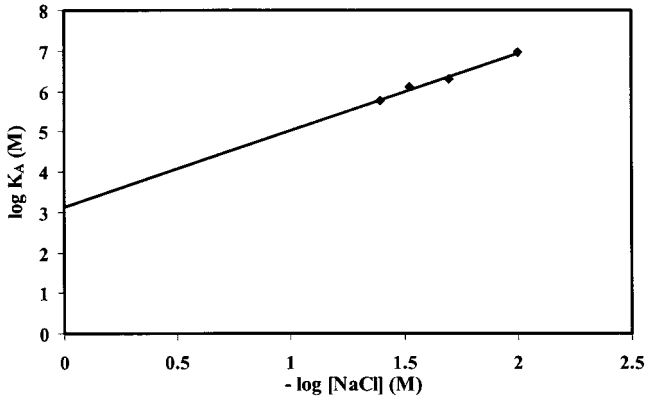

FIGURE 6: Nonelectrostatic free energy of binding of AVP−pVIc to 12-mer dsDNA. Increasing concentrations of AVP−pVIc were added to 10 nM 5′-fluorescein-labeled 12-mer dsDNA in 0.01, 0.02, 0.03, and 0.04 M NaCl at 25 °C. Two minutes after each addition, the change in anisotropy was measured. The data were analyzed to obtain equilibrium association constants, K_A, as described in Materials and Methods.

The nonelectrostatic change in free energy, ΔG_0^0, upon binding of AVP−pVIc to DNA was also calculated. The line in Figure 6 was extrapolated to a Na^+ concentration of 1 M. Then, the following equation was used:

$$\Delta G_0^0 = -RT \ln K_o$$

where K_o is K_A in 1 M Na^+. The ΔG_0^0 (1 M Na^+) was −4.2 kcal. By correction for two lysine-like ion pairs, which have a ΔG_{Lys}^0 (1 M Na^+) of 2 × 0.18 kcal, the nonelectrostatic free energy of binding was calculated to be −4.6 kcal. The K_d values were 111, 489, 786, and 1771 nM in 0.01, 0.02, 0.03, and 0.04 M NaCl. The K_d by extrapolation of the line in Figure 6 to 1 M NaCl was 794 μM.

Potential DNA Binding Sites Revealed in the Crystal Structure of an AVP−pVIc Complex. The three-dimensional structure of the AVP−pVIc complex has been determined (*10*), and a charge-potential map of the surface of the structure reveals several potential DNA binding sites. The AVP−pVIc structure is ovoid with a long groove containing the active site near the blunt end (Figure 7). Inspection of the surface potential of the structure reveals five large clusters of positive charge that range in area from 45 to 65 Å^2. Three of the clusters, labeled a, c, and e, are at the apical end. The blunt end is relatively neutral in charge. The shortest distances between pairs of clusters are ∼24 Å, close to the diameter of double-stranded DNA (20 Å). This implies that some of these clusters may interact with the viral DNA; e.g., the viral DNA could bind between two large clusters. The active site groove is on the opposite side of the molecule from clusters a, c, and e so that DNA binding in these clusters would not occlude the active site.

DISCUSSION

The data presented clearly showed that DNA is a cofactor for the adenovirus proteinase. Enzyme activity was stimulated by DNA. AVP and AVP−pVIc bind to DNA with physiologically relevant K_d values, 63 and 4.6 nM, respectively. The K_d for the binding of AVP−pVIc to 12-mer ssDNA was determined by two different methods. The K_d derived by fluorescence anisotropy experiments was 18.4 nM, and the

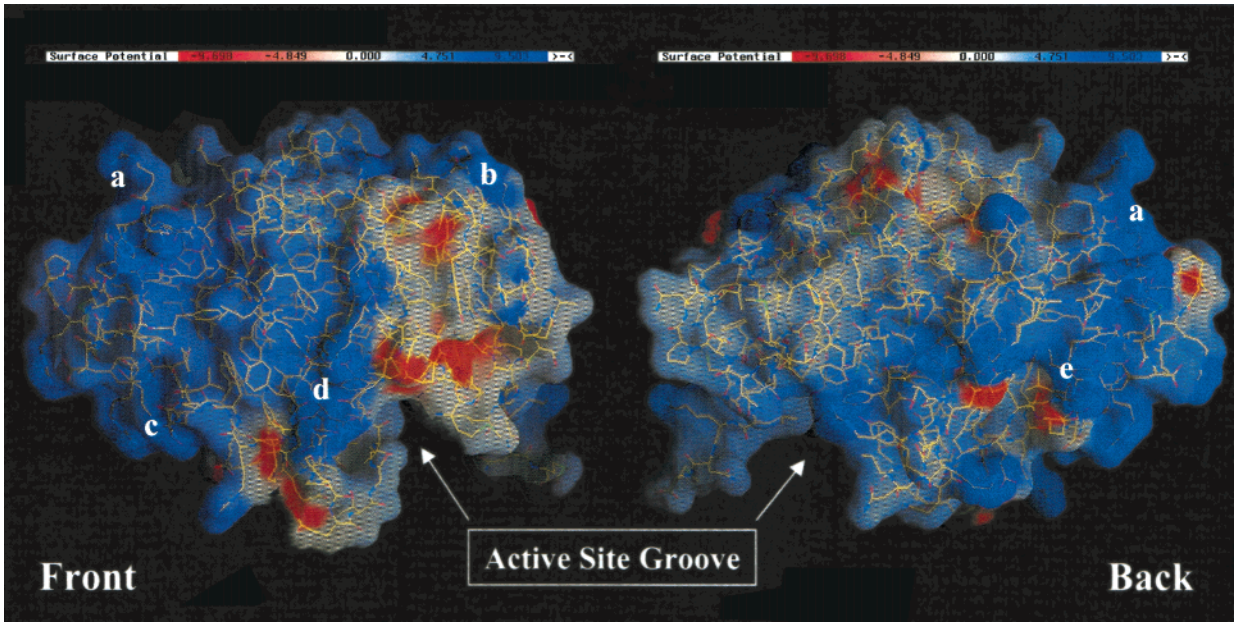

FIGURE 7: Charge-potential map of the distribution of positive and negative charges on the surface of AVP−pVIc. The five positive charge clusters (blue) are labeled a−e, and the arrow indicates the location of the active site groove. Areas colored in red indicate regions of negative charge. The front and back of the molecule are labeled. The figure was generated by the program GRASP (*24*).

K_d derived by enzyme activity measurements was 18.0 nM. When both sets of data were graphed together (Figure 3), the data were superimposable. That implied binding of AVP−pVIc to DNA is coincident with stimulation of enzyme activity. When DNA binds to AVP−pVIc, enzyme activity was stimulated; k_{cat} values increased 10-fold, and K_m values decreased 3-fold.

The binding of pVIc to DNA was not surprising. Five of its 11 amino acid residues are basic. Its isoelectric point is 11.81. The $K_{d(apparent)}$ of 0.69 μM for the binding of pVIc to 12-mer dsDNA may be physiologically relevant. Adenovirus protein VI is a DNA binding protein (*18*). The binding of AVP to DNA and the binding of the C-terminus of pVI to DNA would facilitate the interaction of AVP with pVI to yield pVIc.

The method of analysis used to calculate K_d assumed the stoichiometry of binding of ligand to DNA was 1:1. This was shown to be the correct stoichiometry with 12-mer ds- and ssDNA. The K_d values with other DNAs were all apparent, i.e., $K_{d(apparent)}$, and defined empirically as the concentration of ligand required for half-saturation.

There are several indications that the K_d values for the binding of AVP or AVP−pVIc to DNA are correct. All of the binding curves, obtained either by activity or by fluorescence anisotropy, gave no indication of more than one type of binding reaction. This implied that binding of the enzyme was not occurring preferentially at the ends of the DNA molecules or at nicks in double-stranded DNA. Also, in the fluorescence anisotropy experiments, competition was observed between fluorescein-labeled 18-mer dsDNA and unlabeled 18-mer dsDNA for binding sites on AVP−pVIc. This implied that AVP−pVIc was not binding to the fluorescein moiety on DNA. Measurement of the stoichiometry of binding of AVP−pVIc to 12-mer dsDNA required the concentration of one of the components in the reactions be at least 10-fold higher than the K_d. With 100 nM 12-mer dsDNA, tight binding was exhibited, implying the K_d was less than 10 nM; measurement of the K_d for binding of AVP−pVIc to 12-mer dsDNA yielded a K_d of 2.9 nM. Finally, the K_d values for the binding of AVP−pVIc to 12-mer ssDNA were identical whether determined by enzyme activity or by fluorescence anisotropy.

The physical basis for DNA being a cofactor is that it is a polymer of high negative charge density (*6*). Consistent with this conclusion that the binding of AVP to DNA is not sequence specific are the data on the stoichiometry of binding to DNA. Three AVP−pVIc molecules saturated the binding sites on one 18-mer dsDNA, and six AVP−pVIc molecules saturated the binding sites on one 36-mer dsDNA. On Ad2 DNA, there are about 3027 binding sites.

The two cofactors increased the k_{cat} for substrate hydrolysis and decreased the K_m. The predominant effect of pVIc was on k_{cat}. The k_{cat} for AVP was 0.002 s^{-1}, and this increased 107-fold because of the presence of pVIc, whereas the K_m decreased only 10-fold. The predominant effect of DNA was on K_m. The K_m for AVP was 95 μM, and this decreased 28-fold, compared to an increase in k_{cat} of 11-fold. Together, there is a synergistic effect of the cofactors. The k_{cat} increased 1209-fold, and the K_m decreased 28-fold. Other proteinases bind to DNA (*19*), but only the enzymatic activity of AVP is stimulated by being bound to DNA.

The non-sequence specific interaction between AVP−pVIc and DNA exhibited a substantial dependence on monovalent sodium ion concentration (*12*). This dependence reflects the electrostatic component of the binding reaction (*17*). The electrostatic component originates from the formation of ion pairs between positively charged groups on AVP−pVIc and negatively charged phosphate groups on DNA. After binding occurs, there is a concomitant release of counterions from the DNA and, possibly, from AVP−pVIc. From an analysis of the equilibrium association constants for the binding of AVP−pVIc to 12-mer dsDNA as a function of the Na^+ concentration, an accurate estimate of the number of ion pairs involved in the interaction was obtained. Two ion pairs were involved in complex formation with AVP−pVIc and 12-mer dsDNA. For comparison, two ion pairs of the T4 gene

32 protein are involved in non-sequence specific binding to helical DNA (*17*).

With both proteins, there seems to be a substantial favorable nonelectrostatic component of the binding interaction. Upon extrapolation to 1 M Na^+ of the line in Figure 6, the $\Delta G_0^0 = -4.2$ kcal for AVP−pVIc. The $\Delta G_0^0 = -2.2$ kcal for the gene 32 protein (*17*). Correction for two lysine-like ion pairs makes the nonelectrostatic free energy of binding −4.6 kcal for AVP−pVIc complexes and −2.6 kcal for the gene 32 protein. This indicates that a substantial component of the binding free energy under physiological conditions results from nonspecific interactions between AVP−pVIc and base or sugar residues on the DNA and that the dominant factor driving the nonspecific interaction between AVP−pVIc and DNA is the entropic contribution from the release of counterions.

The data presented here clearly show that AVP and AVP−pVIc were stimulated by DNA. There may be several reasons why Webster et al. (*9*, *15*) did not see stimulation of AVP−pVIc activity by DNA. Using their assay conditions, but with our enzyme and substrate, DNA stimulated the rate of substrate hydrolysis, but only 6.5-fold. Under our conditions, a 43-fold stimulation in the rate of substrate hydrolysis was observed. Factors that influenced enzyme activity under these conditions were the length of time in preincubation of enzyme with cofactor before addition of substrate and the concentrations of substrate, pVIc, and DNA. High concentrations of substrate and DNA can be inhibitory. The DNA stimulation effect could be specific to our rhodamine-based substrates. Their substrate is an octapeptide (*15*). However, when a different group used a rhodamine-based substrate, they observed no stimulation of enzyme activity by DNA (*20*).

DNA binding activates AVP and localizes the enzyme to the DNA. This and other observations have led to a model for the regulation of AVP by its cofactors. AVP is synthesized as a relatively inactive enzyme. The K_m for (Leu-Arg-Gly-Gly-NH)$_2$-rhodamine was 95 μM, and the k_{cat} was 0.002 s^{-1}. If AVP were synthesized as an active enzyme, it would probably cleave virion precursor proteins before virion assembly, thereby preventing the formation of immature virus particles. Consistent with this hypothesis is the observation that if exogenous pVIc is added to cells along with Ad5 virus, the level of synthesis of infectious virus in those cells was severely diminished (*21*, *22*, *25*).

Quite possibly, AVP enters empty capsids bound to the viral DNA and remains bound during the maturation of the virus particle. It enters empty capsids bound to the viral DNA, because the K_d for the binding of AVP to 12-mer dsDNA was quite low (63 nM). Inside the young virion, the viral DNA is positioned next to the C-terminus of virion protein pVI. Protein VI is a DNA binding protein (*18*). AVP is partially activated by being bound to the viral DNA. Compared to the values with AVP alone, the K_m decreased 10-fold and the k_{cat} increased 11-fold. Thus, AVP−DNA complexes can cleave pVI at the proteinase consensus cleavage site preceding the amino acid sequence of pVIc. The liberated pVIc can then bind either to the viral DNA [$K_{d(apparent)} = 693$ nM], to AVP molecules in solution ($K_d = 4400$ nM), or, most likely, to the AVP−DNA complex that liberated it ($K_d = 90$ nM) (*25*). Once pVIc is bound to AVP, the penultimate cysteine in pVIc forms a disulfide bond with Cys104 of AVP (*10*). Now, AVP is permanently activated. Compared to the values with AVP alone, with pVIc−AVP−DNA, the K_m has decreased 28-fold and the k_{cat} increased 1209-fold.

How can 70 fully activated proteinases bound to the viral DNA inside the virion (*4*) cleave precursor proteins 3200 times to render a virus particle infectious? For this to occur, either enzyme or substrate must move inside young virions. Perhaps the proteinase moves along the viral DNA searching for processing sites on precursor proteins such as the *E. coli* RNA polymerase holoenzyme moves along DNA searching for a promoter. AVP−pVIc and RNA polymerase both exhibit an appreciable, non-sequence specific affinity for DNA. The K_d values are 60 and 100 nM, in nucleotide base pairs, for AVP−pVIc and RNA polymerase (*23*), respectively.

RNA polymerase binds to DNA via a two-step mechanism. Initially, RNA polymerase binds to any place on DNA via free diffusion in three-dimensional space. Next, it dissociates from the DNA to a point where, though free to move, it is still near the original binding site. This enables it, with high probability and within a short period of time, to reassociate with the same or a nearby binding site. Once it locates a promoter, it exhibits an enormous affinity for that sequence ($K_d = 10$ fM in nucleotide base pairs) (*23*). Because of "nonspecific" binding, the search process for the promoter in the second step occurs in reduced dimensionality or volume. That is how RNA polymerase can reach a promoter at a rate faster than a diffusion-controlled rate; diffusion is occurring in one dimension.

In the case of AVP, perhaps the viral DNA serves as a scaffold next to which reside the 3200 processing sites that must be cleaved. The 70 AVP−pVIc complexes could then move along the viral DNA via one-dimensional diffusion, using the DNA as a guide wire in cleaving precursor proteins. By using the viral DNA as a guide wire, AVP could quickly (via one-dimensional diffusion) and efficiently (by the alignment of the cleavage sites near the DNA and by moving along the DNA) process the numerous virion precursor proteins.

The utilization of DNA as a cofactor for a proteinase activity is unprecedented. DNA is a cofactor for the proteinase in the virus particle (*6*). In disrupted ts-1 virus, proteinase activity can be detected upon the addition of AVP. However, if disrupted virus particles are treated with DNase and then AVP is added, no proteinase activity can be detected. Treatment of disrupted ts-1 virus with DNase, inactivation of the DNase, and addition of DNA followed by AVP resulted in restoration of proteinase activity. Additionally, in disrupted ts-1 virions, the precursor proteins are processed upon incubation with AVP. However, no processing occurs if disrupted ts-1 virions are pretreated with DNase before the addition of AVP (*12*). Here AVP and AVP−pVIc were shown to bind tightly to DNA, and stimulation of proteinase activity by the presence of DNA was coincident with binding to DNA.

REFERENCES

1. Weber, J. (1976) *J. Virol. 17*, 462−471.
2. Hannan, C., Raptis, L. H., Dery, C. V., and Weber, J. (1983) *Intervirology 19*, 213−223.

3. Mirza, A., and Weber, J. (1980) *Intervirology 13*, 307−311.
4. Brown, M. T., McGrath, W. J., Toledo, D. L., and Mangel, W. F. (1996) *FEBS Lett. 388*, 233−237.
5. Yeh-Kai, L., Akusjarvi, G., Alestrom, P., Pettersson, U., Tremblay, M., and Weber, J. (1983) *J. Mol. Biol. 167*, 217−222.
6. Mangel, W. F., McGrath, W. J., Toledo, D. L., and Anderson, C. W. (1993) *Nature 361*, 274−275.
7. Tihanyi, K., Bourbonniere, M., Houde, A., Rancourt, C., and Weber, J. M. (1993) *J. Biol. Chem. 268*, 1780−1785.
8. Anderson, C. W. (1993) *Protein Expression Purif. 4*, 8−15.
9. Webster, A., Hay, R. T., and Kemp, G. (1993) *Cell 72*, 97−104.
10. Ding, J., McGrath, W. J., Sweet, R. M., and Mangel, W. F. (1996) *EMBO J. 15*, 1778−1783.
11. McGrath, W. J., Abola, A. P., Toledo, D. L., Brown, M. T., and Mangel, W. F. (1996) *Virology 217*, 131−138.
12. Mangel, W. F., Toledo, D. L., Brown, M. T., Martin, J. H., and McGrath, W. J. (1996) *J. Biol. Chem. 271*, 536−543.
13. Gill, S. G., and von Hippel, P. H. (1989) *Anal. Biochem. 182*, 319.
14. Jensen, D. E., Kelley, R. C., and von Hippel, P. H. (1976) *J. Biol. Chem. 251*, 7215−7228.
15. Webster, A., Leith, I. R., and Hay, R. T. (1994) *J. Virol. 68*, 7292−7300.
16. Spencer, R. D., and Weber, G. (1969) *Ann. N.Y. Acad. Sci. 158*, 361−376.
17. Record, M. T., Lohman, T. M., and De Haseth, P. (1976) *J. Mol. Biol. 107*, 145−158.
18. Russell, W. C., and Precious, B. (1982) *J. Gen. Virol. 63*, 69−79.
19. Joshua-Tor, L., Xu, H. E., Johnston, S. A., and Rees, D. C. (1995) *Science 269*, 945−950.
20. Diouri, M., Geoghegan, K. F., and Weber, J. M. (1995) *Protein Pept. Lett. 2*, 363−370.
21. Rancourt, C., Keyvani-Amineh, H., Sircar, S., Labrecque, P., and Weber, J. M. (1995) *Virology 209*, 167−173.
22. Ruzindana-Umunyana, A., Sircar, S., and Weber, J. M. (2000) *Virology 270*, 173−179.
23. Hinkle, D., and Chamberlin, M. (1972) *J. Mol. Biol. 70*, 187−196.
24. Nicholl, A., and Honig, B. J. (1991) *J. Comput. Chem. 12*, 435−445.
25. Baniecki, M. L., McGrath, W. J., McWhirter, S. M., Li, C., Toledo, D. L., Pellicena, P., Barnard, D. L., Thorn, K. S., and Mangel, W. F. (2001) *Biochemistry* (in press).

BI0111653